Extracting absorption coefficients from a room impulse response using a convolutional neural network with domain adaptation

T.T.J. Bloemen[1]

Supervisors: J. Martinez Castaneda, D. de Groot

[1]EEMCS, Delft University of Technology, The Netherlands

A Thesis Submitted to EEMCS Faculty Delft University of Technology,
In Partial Fulfilment of the Requirements
For the Bachelor of Computer Science and Engineering
June 23, 2024

Name of the student: T.T.J. Bloemen
Final project course: CSE3000 Research Project
Thesis committee: J. Martinez Castaneda, D. de Groot, S. Pera

***Abstract*—In building design, it is important to consider certain materials for certain acoustical properties. Specifically, the time it takes for an audio signal to decrease in volume by 60 dB is important. This can be estimated with Sabine's and Eyring's formula's, which both make use of the average absorption coefficient of the materials in a room. This absorption coefficient indicates how much of the original audio signal is absorbed into the material. However, measuring these absorption coefficients for a material is difficult and time consuming. In this study, a machine learning approach is used to estimate the absorption coefficients, by using the room impulse response in combination with the layout of a room. A room impulse response is the characterizing sound of a room. These two pieces of data are processed through a convolutional neural network and a multilayer perceptron, respectively, and combined to make the final prediction of absorption coefficients. A novel approach of simulating the data is used, and a real dataset is used in conjunction with the simulations to use a state-of-the-art regression loss function made for domain adaptation. The results show that the machine learning approach still has a large error compared to using Eyring's formula, and that machine learning is not yet a viable option to use instead of conventional methods.**

***Index Terms*—Room impulse response, machine learning, acoustical parameters, absorption coefficient, domain adaptation.**

I. Introduction

In building design, it is important to take the acoustics of your building into account. Among other articles in the building regulations in the Netherlands, there are certain standards a building has to meet, such as a sound decrease of at least 20 dB with respect to the outside world [1]. In order to comply with these standards, careful selections have to be made, as making a wall too thin or out of the wrong material could lead to not complying to the Building Regulations.

A major component in determining the acoustic quality in a room, are the absorption coefficients of the walls, floor and ceiling in a room. These can be used to calculate certain properties of the room, such as the decay time it takes for a signal to diminish 60 dB below the original sound, otherwise known as the T_{60} or RT_{60} [2]. In current building acoustics, Sabine's reverberation equation is used to estimate the $T_{60}(f)$, given the room volume and surface area, and the absorption coefficients, assuming room temperature at 20 degrees Celsius.

$$T_{60}(f) = 0.163\frac{V}{S\overline{\alpha}(f) + 4mV} \tag{1}$$

where V is the volume of the room, S is the surface area of the room, m is an air attenuation constant and $\overline{\alpha}(f)$ is the average absorption coefficient of the room as a function of frequency [2]. For small rooms, the term $4mV$ (air attenuation) can be ignored due to it's small size. More specifically, $\overline{\alpha}(f)$ is defined as

$$\overline{\alpha}(f) = \frac{1}{S}\sum_i S_i\alpha_i(f) \tag{2}$$

where $\sum_i$ counts all the surfaces in a room, and S_i, α_i are the surface area and absorption coefficient of that surface. However, $\alpha(f)$ is a frequency dependent property of a surface. This means the room surfaces can impact the sound or character of a room.

Depending on the use case, it is vital to know the absorption coefficients at certain frequencies. When making a concert hall, one might want to aim for a different T_{60} in the high frequency range than in a classroom. However, these values are not known for all materials, and still remains a challenge to calculate [3].

Currently, the state of the art formula for calculating the T_{60} formulaically is Eyrings formula, which is a more exact decay formula than Sabines formula (Eq. (1)) [2].

$$T_{60}(f) = -0.163\frac{V}{S\ln(1-\overline{\alpha}(f)) + 4mV} \tag{3}$$

where $\overline{\alpha}(f)$ is calculated from equation (2), and again, the air attenuation can be ignored. This equation can be rewritten to extract the absorption coefficient from a known $T_{60}(f)$:

$$\overline{\alpha}(f) = 1 - \exp\left(-0.163\frac{V}{ST_{60}(f)}\right) \tag{4}$$

However, this estimation is not perfect, as the actual T_{60} of equation 3 can vary by $\pm 10\%$ [4]. In this study, the following research question arises:

> Can a machine learning approach estimate the absorption coefficient better than the inverted Eyring's formula? Specifically, can an augmented data approach be applied to a ML model in combination with a state-of-the-art approach to domain adaptation for regression problems [5]?

A. Related work

Parameter extraction based on room impulse responses is an active field of study. However, just as there is research on parameter extraction, there are studies which simulate room impulse responses based on parameters. A commonly used method is the Image Source Method [6], which uses the idea that you can model the reflections in a room as virtual sources beyond the walls of the room. The more virtual sources are used to model the real reflections, the more accuracy can be achieved. The amount of reflections against a wall, or similarly said, the amount of times a virtual source passes through a wall, is called the reflection order. This method is computationally expensive, and this has lead to research to optimize these simulations [7], [8]. More recent work tries to achieve higher reflection orders and high accuracy, especially in the lower frequencies [9]. Ray-tracing approaches are also being used, with recent advancements using hardware ray-tracing [10]. Another method is proposed using kernel regressions methods [11], [12]. There are also data driven approaches to RIR simulation, such as in [13] and [14]. This approach has the advantage of not needing assumptions about sound wave propagation, acoustic environment or measuring setting. The realism of simulations is also tested. It has been shown that different T_{60} approximation formula's, such as Sabine's or Eyring's, have different errors for different scenario's [15].

Similar to room impulse response generation, there are also multiple approaches to parameter extraction [16]–[18]. Multiple studies have been done regarding absorption coefficient

estimation through different means, such as a geometry based estimation [19], and machine learning [20]–[22]. The main differences between machine learning studies on absorption coefficient extraction can be seen in:

1) If the estimation is blind [18], [21]–[23] or augmented with data [19], [24].
2) The type of machine learning model applied (e.g. a convolutional neural network [21], [23]–[25], a multi layer perceptron [23], [24], or other [18], [19]).
3) If the estimation is on simulated datasets only [19], [21], [22], [24] or also on real RIR's [18], [23].
4) If the room size is fixed [24], or is varied throughout the training process [18], [19], [22], [23], [26].
5) If the parameters are extracted from just the RIR [19], [22]–[24], or audio convolved with the RIR [18], [21].
6) If the RIR is multichannel [26] or single channel [18], [19], [22]–[24].
7) If the absorption coefficients are estimated per wall [19], [22], [24] or as an average [23], [26].
8) If the absorption coefficients are estimated as a function of frequency [19], [22]–[24], and if yes, which frequency bands are used.

In Section II the methodology of the study is explained, followed by Section III on responsible research. Next, we discuss the results of the study in Section IV, and draw conclusions on the experiment in Section V.

II. Methodology

The absorption coefficient estimator developed in this paper is restricted to only shoe box-type rooms, that is rectangular rooms with a length, width and height. This is chosen because of the relatively low complexity level for the simulator, and more options for the real data, as the recordings of real RIR's are predominantly made in shoe box-type rooms. The machine learning model used for the estimation is summarized in figure 1. The model has two inputs: the input of the room impulse response (RIR) and the input of the numerical data. Having additional data outside of the RIR itself makes this an estimator with augmented data instead of a blind estimator. The room layout data provided are the dimensions of the room (L_x, L_y, L_z), the position of the microphone (M_x, M_y, M_z) and the position of the speaker (S_x, S_y, S_z). These values were chosen because of the relative ease of getting this information in a real-world setting, as it is straightforward to accurately measure your the distances of your equipment and dimensions.

The output of the model corresponds to the 10 frequency bands considered in this study. These bands were determined as follows: The range of human hearing is standardized as 20-20000 Hz [27]. In architecture, common convention is to measure the absorption coefficient in octave bands, centered around 1000 Hz. Extrapolating this to fit to the hearing range, the frequency bands' centers are 31.25, 62.5, 125, 250, 500, 1000, 2000, 4000, 8000 and 16000 Hz. For each of these centers, the band contains the frequency of a square root below it, and a square root above it, due to it being an octave band.

The microphone and speaker placement is done by ensuring the position is at least 0.5 meter away from any surface, and at least 1 meter from each other [28].

A. Preprocessing

All RIR's undergo preprocessing to have standardize all inputs. First, every RIR is resampled to 48 kHz. Then, the response is normalized, and convolved with a bandpass filter, to isolate the frequencies of that band. A Butterworth filter is chosen for this task with 5 poles, as a Butterworth filter provides a maximally flat frequency response in the passband [29], which in this case, is the octave band we are trying to measure. After the RIR has been split into frequency bands, the length of the RIR is set to 1 second. 1 second has been chosen because it keeps the number of inputs for the model low, and most of the real data has a T_{60} below 1 second (figure 2). The RIRs are then saved to file, and their filename with the room layout data is written to a csv file.

B. Layer design

The RIR response is going through a convolutional neural network (CNN), as the current literature suggests better performance for CNN's as opposed to multi layer perceptrons (MLP's) in the context of absorption coefficient estimation [24]. The layer design is visualised in figure 1. To expand upon the existing research, the CNN layer design is very similar to the existing literature [24], [23]. There are 3 one-dimensional convolutional hidden layers with output channels of size 64, 32, 16 and kernel size 33, 17, 9 respectively. After each layer is a ReLU, batch normalization [30] and a Maxpooling layer of size 4. This results in 16 channels with 746 numbers, which then goes into a fully connected layer with 125 outputs. This is then reshaped into 1 layer of 2000 outputs.

The room layout data goes through a relatively simple MLP with two fully connected layers: from 9 to 64, and from 64 to 500.

Together, the RIR data and room layout data are concatenated to the same feature space, where the first 2000 logits of information come from the RIR and the last 500 logits come from the numerical data. This goes into a fully connected layer with an output of 500 channels, which are in turn fully connected into 10 outputs, which corresponds to the absorption coefficient per frequency band.

C. Loss functions

The loss function calculation is summarized in figure 1. The feature space is the space with which the DAREGRAM loss [5] is calculated. The DAREGRAM loss is a loss function for domain adaptation in regression problems. Summarized, it computes a measure of similarity from the feature space Z between real data and simulated data. It does this by computing the Gram matrix $(Z^T Z)^{-1}$ of both the simulated data and the real data, and tries to align features in that space by measuring the cosine simularity of that space and the scale simularity. The representation of the feature space as a Gram matrix is motivated by the ordinary least squares closed form, as seen in equation 5 which uses that same representation.

$$\hat{\beta} = (Z^T Z)^{-1} Z^T Y \tag{5}$$

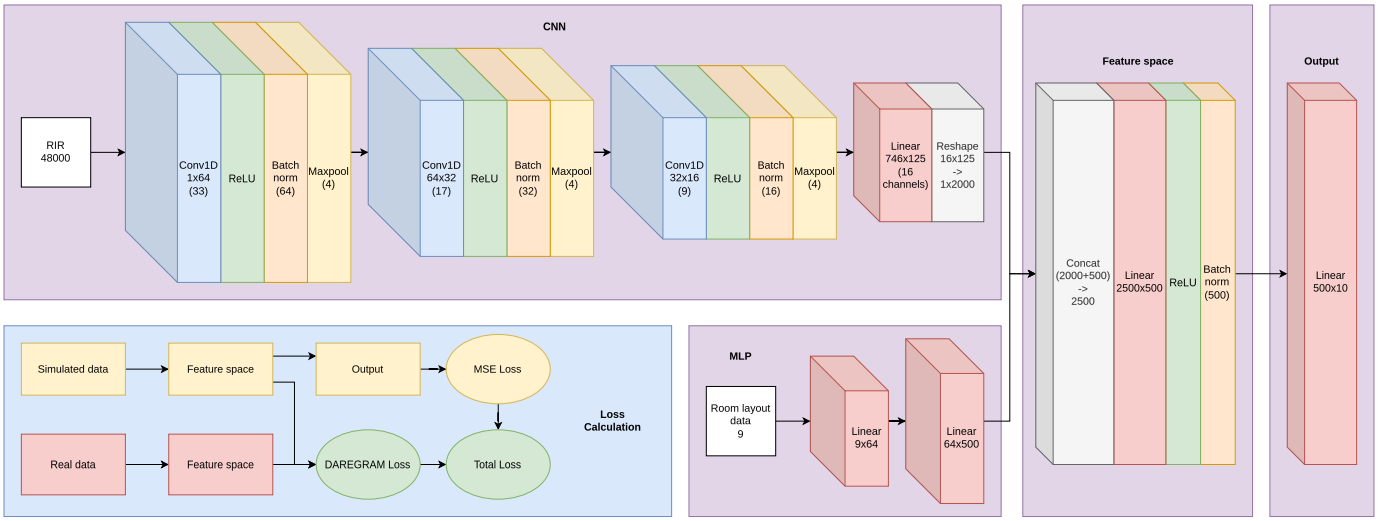

Fig. 1. The layout for the machine learning model. This model combines the audio signal of the room impulse response with the room layout data. The layers consist of a CNN for the input data, a MLP for the room layout data, and finally the mapping to the feature space and the output layer. In the bottom left, the loss calculation is pictured: The model trains with DAREGRAM loss [5], which tries to minimise the difference at the feature space layer. From there, the model estimates the absorption coefficient in the output layer. The total loss is equal to the DAREGRAM loss plus the MSE loss.

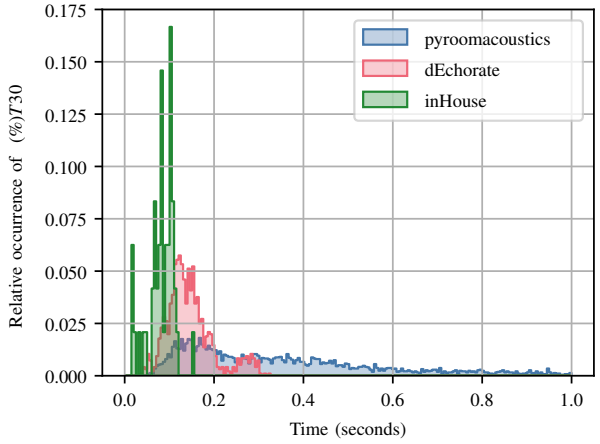

Fig. 2. The distribution of decay times per dataset. For this graph, the T_{30} was measured for all recordings, and plotted as a histogram. These amounts are normalized, which means that the histograms for each dataset are rescaled so the area under all these graphs is equal to 1.

where $\hat{\beta}$ are the optimal coefficients, Z is the feature space, and Y is the output. The DAREGRAM loss is complemented with a main loss function. For regression problems, the mean absolute error (MAE), the mean squared error (MSE) and the root mean squared error (RMSE) loss functions are regarded as standard loss functions for regression problems. However, there is no clear consensus on which loss function is better in general, as it also depends on the input data [31]. The MAE is defined as follows:

$$\mathcal{L} = \frac{1}{n}\sum_{i=1}^{n}|Y_i - \hat{Y}_i| \tag{6}$$

where $\mathcal{L}$ is the loss, n is the length of all data points in a batch, Y is the actual output, and $\hat{Y}$ is the predicted output. Similarly, the MSE is the error squared:

$$\mathcal{L} = \frac{1}{n}\sum_{i=1}^{n}|Y_i - \hat{Y}_i|^2 \tag{7}$$

And the final loss function takes the square root of the entire expression:

$$\mathcal{L} = \sqrt{\frac{1}{n}\sum_{i=1}^{n}|Y_i - \hat{Y}_i|^2} \tag{8}$$

For this study, initially the MAE was chosen, as research indicates that this loss function can perform better than the MSE in deep neural network-based vector-to-vector problems [32]. However, a vector of length 10 is not necessarily the same as the vector size in this paper, so for completeness, the same model has also been trained on the MSE and the RMSE. The MAE had a significantly worse outcome, with a final MAE error of 0.47, while the MSE and RMSE gave much lower similar results, which are discussed in Section IV. Since the results of the RMSE and the MSE were so similar, the choice of loss function was arbitrary between the two. The MSE was ultimately chosen.

D. Real data

For real data, the dEchorate dataset was used [33]. This dataset was chosen because of the fact that absorption coefficient estimation has been done on this dataset earlier [23], it is recent, and has correct room layout data.. Only the omnidirectional sources were used in this study, as directional speakers add another layer of complexity. Furthermore, the numerical data doesn't include the direction of the microphone, so this would add a degree of blindness which is unnecessary. Ideally, the RIR is the same no matter which directivity the speaker has. This would mean that the measuremnts of a RIR are more reproducable [34]. This has been formalized in the current acoustic standards [35].

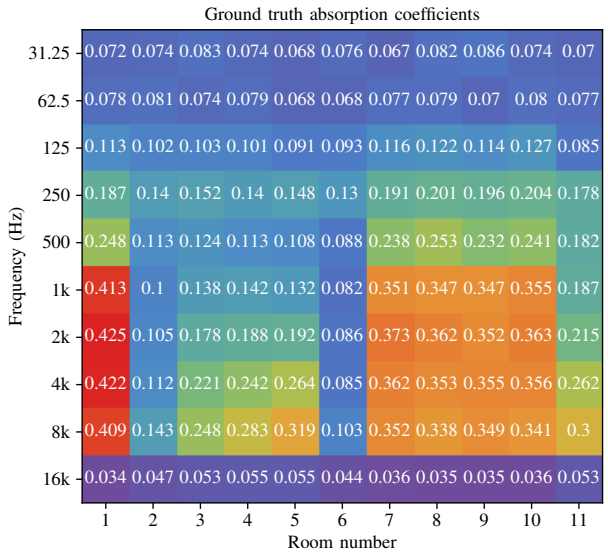

Fig. 3. The ground truth from an aggregation of applying formula 4. On the vertical axis, the center of the frequency bands is displayed, with the room number on the horizontal axis. In the dEchorate dataset, the room number corresponds to a specific configuration of the room.

The ground truth of the absorption coefficients is not annotated with the dEchorate dataset, or with any dataset of real RIRs to the best of our knowledge. Instead, we will estimate the absorption coefficient by acquiring the average absorption coefficient generated by equation 4 as the absorption coefficient should be the same in each room configuration of the dEchorate dataset, regardless of where the source and receiver are placed. This approach is the same as used in [23].

To achieve the average absorption coefficient per frequency band, the $T_{60}(f)$ therefore necessary from the RIR's. This is calculated using the Schroeder curve [36]. After splitting the RIR into octave bands (see Section II-A), the T_{60} is estimated using this curve. Because the amplitude of the RIR is not always large enough to measure 60 dB's of difference, a tradeoff has been made. The compromise is to estimate the T_{30} if possible, and if this isn't possible, the T_{20} is estimated. Finally, if that is not possible, the T_{15} is estimated. This is an approximation, as in general, $T_{60} \neq 2T_{30} \neq 3T_{20} \neq 4T_{15}$. However, these lower decay times can estimate the T_{60} if the decay curve is log-linear. In general, the noise floor in the dEchorate dataset is below 60 decibels, as can be seen in figure 8, but not by a lot. If the noise floor is at -45 dB or lower, the T30 is recommended [37] [28]. For this reason, the T_{30} was chosen as the starting point for the estimation.

In contrast to the values achieved by [23], only omnidirectional sources were considered in the aggregation of absorption coefficients. Therefore, the values of ground truth are slightly different. This results in the ground truth table visualized in figure 3.

E. RIR Simulation

For the simulated data, the library pyroomacoustics [38] is used. This library was chosen for the reason that it has the option to specify the absorption coefficient per wall, per frequency band, as opposed to other implementations such as gpuRIR [39] or Habets [40]. This uses a reflection coefficient, which is defined as the complement to 1 of the absorption coefficient:

$$\beta = 1 - \alpha \tag{9}$$

where β is the reflection coefficient, and α is the absorption coefficient. Written in this form, these are not frequency-dependent values, rather they are complex values, so $\alpha, \beta \in \mathbb{C}$. The frequency response is translated into the phase of these quantities. Pyroomacoustics has no implementation for complex-valued reflection coefficients, or absorption coefficients, but rather chooses the approach of specifying the absorption coefficients in the frequency domain. This way, the frequency specific behaviour of a material is preserved, in a similar manner to how gpuRIR can implement frequency specific behaviour in the time domain. While the complex valued reflection coefficient specified in such an implementation can be derived from the magnitudes of the absorption coefficient per octave band, this was deemed outside of the scope of this paper.

The dimensions of the room are uniformly sampled within predetermined bounds: $L_x \in [4, 10]$, $L_y \in [2, 10]$, $L_z \in [2.5, 5]$, where are the units are in meters. The materials for a surface are constructed with the dimensions of the surface and the absorption coefficient.

In this study, the original method was to base the simulated surface material on real rooms, but to the best of our knowledge, there is no data with the current material usage of buildings. There is a standardized dataset for some building materials [41], however this contains too little information about which materials are on which surface in a room, which is essential information for the proper modelling of the absorption parameters. As a compromise, we implement the reflection biased technique from [23]. This technique approximates real rooms by modeling each surface as either an absorbent surface or reflective surface. For each surface, the chance of the surface being reflective is set to $p = \frac{1}{2}$.

If the surface is reflective, the surface absorption parameter is sampled from the reflective surface profile. The materials with an average absorption coefficient $\overline{\alpha} \leq 0.15$ are considered to be reflective, as most of the materials could be easily be placed above or below this threshold, but future research could potentially improve realism by evaluating if 0.15 is a good threshold value.

If the surface is absorbent, the absorption coefficient is sampled from the absorbent material profile per surface. This is also frequency dependent, so for each octave band, a maximum and a minimum value are chosen. In contrast to the reflection biased sampling method of [23], the absorption profile is extended to all the frequency bands of human hearing, by keeping the same minimum and maximum absorption coefficient of the lowest frequency band for all frequency bands lower than that. Similarly, the frequency bands higher than the highest known frequency band have the same minimum and maximum absorption coefficient.

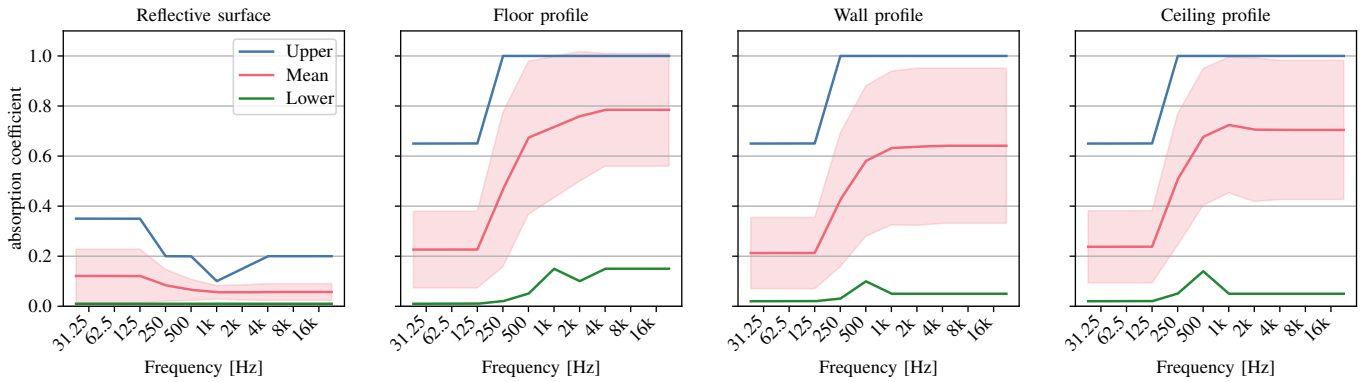

Fig. 4. The absorption profiles per type of surface. The upper bounds, lower bounds, and mean value are plotted against the frequency bands. The blue stroke is one standard deviation above and below the mean.

The distributions for the reflection biased sampling method can be seen in figure 4. It is worthy to note that the profiles of the 92 materials in the paper of [23] do not have a source. This means these numbers are difficult to reproduce, as we don't know which materials were placed into which category. To remedy this, the same approach was recreated by using a materials dataset with more materials [42], and this full dataset can be found in the appendix. Some parts of the data were not included, for various reasons. Moreover, some materials fall into multiple categories, such as glass wool, which can be used for all types of surfaces. The reasons for excluding some data points or the categorization into one or multiple categories is also annotated and available in the appendix.

Instead of sampling uniformly between the maximum and minimum value, the distribution is sampled with a truncated normal distribution. The reason for this is because the maximum and minimum values for absorption coefficients is in a large range, which could give rise to the problem encountered in [22], where the data still was not realistic due to the large sampling window. In an effort to improve the realism of the simulations, the mean and standard deviation of the data points was calculated, and the simulated data now samples with a truncated normal distribution. This does assume that all the materials in the material database are used for buildings in an equal quantity, which might not be the case.

The simulated room impulse responses are made with the presumption that the room is empty. In real life, that is often not the case. However, the real dataset which is used as a reference, is also nearly empty. This means the estimator is trained to be more alike to the real dataset. Picking a dataset with objects in the room is reflected on in section V-A.

III. Responsible Research

This study, the datasets used, the data generated and the code to create the results will all be publicly accessible. No proprietary software or hardware has been used in the making of this study. All results of the data are included. The software, written in python, has been provided with ample comments. Generating new results can be done with a single command. More technical information about the software is written in the 4TU repository [1]. The code base has an MIT license, as the dEchorate dataset also has an MIT license. All plots were made with colors from Paul Tol [43] which are designed to have enough contrast for people with colourblindness. To the best of our knowledge, the findings in this study can not be used for malicious applications.

IV. Results

To answer the research question, it is best to verify the performance of the model with a second real dataset. This dataset has been recorded in a near empty room by supervisor D. de Groot, with approximate room layout data. The dataset is not yet finished, but has enough information for validating my model. Something to note is that these room impulse responses were made with directional loudspeakers, which isn't what the model has trained on. For this study, it has been given the name inHouse, as it was made in house.

The absorption coefficient of the final simulated dataset is plotted in figure 5, against the absorption coefficient of the dEchorate dataset, and the inHouse dataset. The absorption coefficient of the simulated data is on average way higher than that of the dEchorate dataset, and the standard deviation is as well. What is also noteworthy, is that the 16k frequency band has quite low absorption coefficients.

After 500 epochs, the result against the dEchorate dataset can be seen in figure 6. The results have been plotted as a boxplot, per frequency band, against the absolute error on the vertical axis. The estimator developed in this study has quite a large error, especially in the frequency bands of 31.25, and 16000 Hz, as compared to the Eyring error. If we compare these results to the state of the art, we can see the estimator performs worse than the estimator of Yu, W [22]. The RMSE for full band RIRs averages at 0.09, while this estimator has an RMSE of 0.18. In [23], the MAE achieved per room on average is more or less 0.17, as read from figure 9 in that research. This includes only error from octave bands with center frequencies 500, 1000, 2000, and 4000 Hz. For these frequencies, the accuracy of the model in this paper is 0.123.

[1]The DOI of the code base is 10.4121/220c9304-6a1e-44c6-8c8b-f3a7b635d418

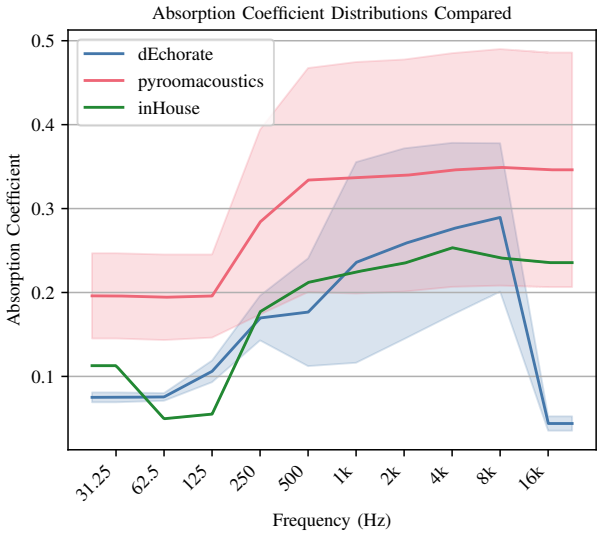

Fig. 5. The distribution of the absorption coefficients from the dEchorate dataset, the simulated dataset, and the inHouse dataset. The mean absorption coefficient per frequency is plotted, the band around the lines is one standard deviation away from the mean. The inHouse dataset doesn't have any bands, as it is recorded in a single room.

V. Conclusions

The answer to the research question is that the estimator indeed can estimate the absorption coefficients, but it doesn't perform nearly as good as the Eyring error. This can be attributed to the choice of real dataset: Among the research group, it was anecdotally found that the room impulse responses of the dEchorate dataset sounded different from other room impulse responses. This might be attributed to the relatively high amplitude in the lower frequencies. There are however, to the best of our knowledge, no other datasets available which correctly annotate the room layout. It is possible that the ML model error becomes lower if a different real dataset is used, or if an aggregation of datasets is used.

What is probably a larger difference, is the difference in T_{60} times between the datasets. The simulated dataset has on average a longer T_{60} and is distributed very evenly among the decay times, while the real data has a much lower decay time, as can be seen in figure 2.

Another possible attribute to high errors is the simulation software used. If there is not enough essential information in the simulated dataset, the model cannot accurately estimate the absorption coefficients. The results could be different if a different simulator is used such as Habets [40]. However, as mentioned in Section II-E, it was out of scope for this project to create our own function which transforms the octave band absorption coefficients to the proper time-domain reflection coefficients.

A. Future work

This model shows that even when using state-of-the-art machine learning techniques, the models for absorption coefficient estimation are still not accurate enough. Some next steps in this field could be to try a similar machine learning setup, but trying different deep learning models, instead of CNN's and MLP's. Different auxiliary data could be supplied, such as only the room volume for instance. This would be easier to set up, as the locations of the speaker and microphone don't need to be annotated. Additionally, there are more datasets which can be used and rooms with an arbitrary shape could be evualated by this metric. To increase the realism of the model, a promising result could be had for choosing and simulating RIR datasets with furniture and people inside the room. Lastly, for this model specifically, more real datasets could be made to train this network, which could make it more accurate. A more realistic threshold value for the reflective surfaces could be determined, or a different ratio of reflective to non-reflective. The optimal hyperparameters for such a project is also something that could be exhaustively tested.

References

[1] *Besluit bouwwerken leefomgeving*, 2024. [Online]. Available: https://www.bblonline.nl/docs/wet/bbl/hfd4/afd4.3/par4.3.1 (visited on 05/06/2024).

[2] H. Kuttruff, *Room Acoustics Fifth Edition*, Fifth. Spon Press, 2009, ISBN: 9780367870997.

[3] E. Brandão, A. Lenzi, and S. Paul, "A review of the in situ impedance and sound absorption measurement techniques," *Acta Acustica united with Acustica*, vol. 101, no. 3, pp. 443–463, May 2015, ISSN: 18619959. DOI: 10.3813/AAA.918840. [Online]. Available: https://www.researchgate.net/publication/275062283_A_Review_of_the_In_Situ_Impedance_and_Sound_Absorption_Measurement_Techniques.

[4] K. Prawda, S. J. Schlecht, and V. Välimäki, "Calibrating the Sabine and Eyring formulas," *The Journal of the Acoustical Society of America*, vol. 152, no. 2, pp. 1158–1169, Aug. 2022, ISSN: 0001-4966. DOI: 10.1121/10.0013575. [Online]. Available: /asa/jasa/article/152/2/1158/2838408/Calibrating-the-Sabine-and-Eyring-formulas.

[5] I. Nejjar, Q. Wang, and O. Fink, "DARE-GRAM : Unsupervised Domain Adaptation Regression by Aligning Inverse Gram Matrices," pp. 11 744–11 754, Mar. 2023. DOI: 10.1109/cvpr52729.2023.01130. [Online]. Available: https://arxiv.org/abs/2303.13325v1.

[6] J. B. Allen and D. A. Berkley, "Image method for efficiently simulating small-room acoustics," *Journal of the Acoustical Society of America*, vol. 65, no. 4, pp. 943–950, 1979, ISSN: NA. DOI: 10.1121/1.382599.

[7] E. A. Lehmann and A. M. Johansson, "Prediction of energy decay in room impulse responses simulated with an image-source model," *The Journal of the Acoustical Society of America*, vol. 124, no. 1, pp. 269–277, Jul. 2008, ISSN: 0001-4966. DOI: 10.1121/1.2936367. [Online]. Available: /asa/jasa/article/124/1/269/903076/Prediction-of-energy-decay-in-room-impulse.

[8] E. A. Lehmann and A. M. Johansson, "Diffuse Reverberation Model for Efficient Image-Source Simulation of Room Impulse Responses," *IEEE Transactions on Audio, Speech, and Language Processing*, vol. 18, no. 6,

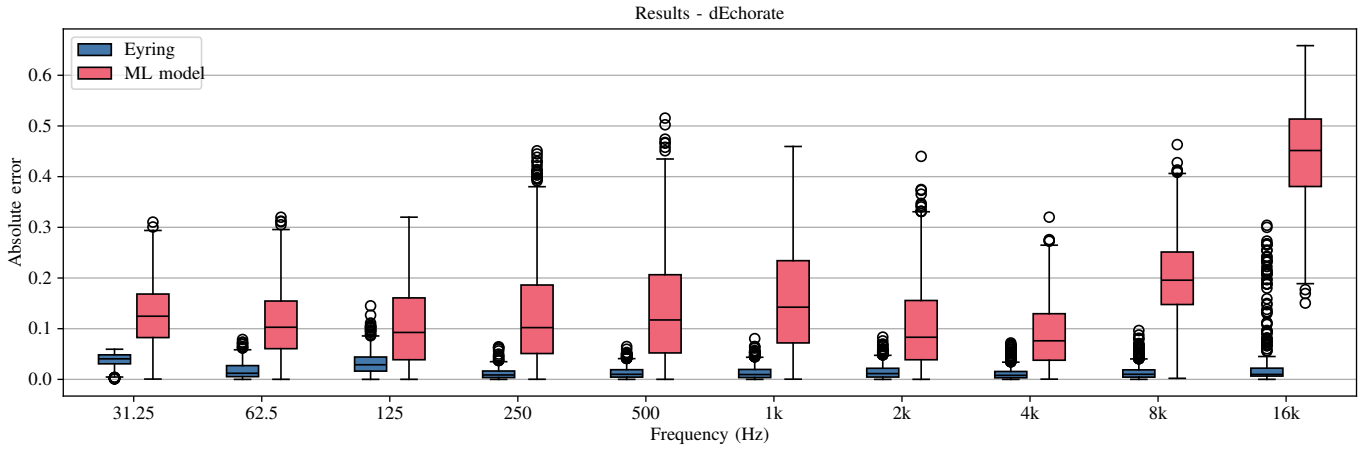

Fig. 6. The absolute error of the machine learning model against the dEchorate dataset, plotted per frequency band. The results are presented as a boxplot. The mean absolute error is 0.161

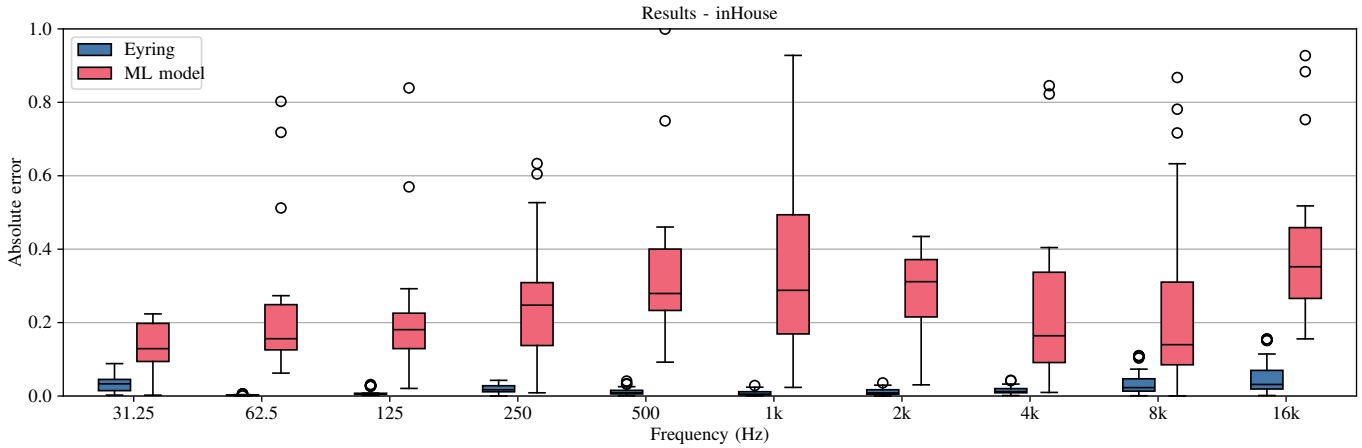

Fig. 7. The absolute error of the ML model against the inHouse dataset, plotted per frequency band. The results are presented as a boxplot. There are some outliers with an MAE above 1, these are not plotted for readability. The mean absolute error is 0.441.

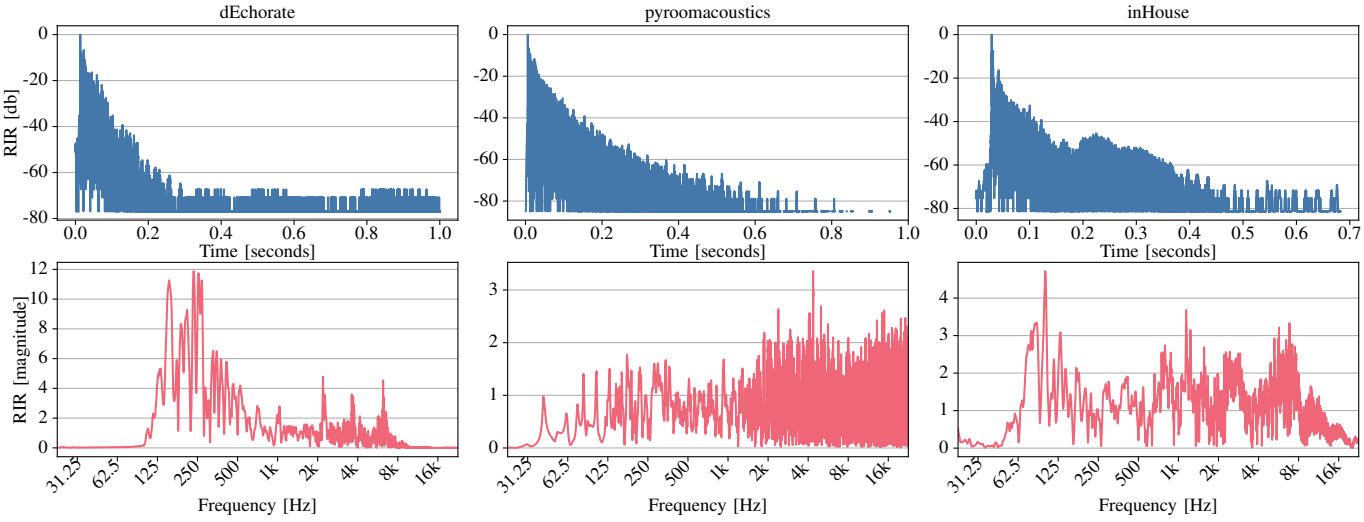

Fig. 8. These are some example room impulse responses plotted out in the time and frequency domain. From left to right, an arbitrary RIR from the dEchorate, pyroomacoustics, and inHouse dataset are shown. The RIR signal in the time domain is plotted in dB, and normalized to the peak level being 0. The frequency response is plotted on a logarithmic scale.

pp. 1429–1439, Aug. 2010, ISSN: 1558-7916. DOI: 10.1109/TASL.2009.2035038. [Online]. Available: http://ieeexplore.ieee.org/document/5299028/.

[9] M. Aretz, P. Dietrich, and M. Vorländer, "Application of the mirror source method for low frequency sound prediction in rectangular rooms," *Acta Acustica united with Acustica*, vol. 100, no. 2, pp. 306–319, Mar. 2014, ISSN: 16101928. DOI: 10.3813/AAA.918710.

[10] P. Thoman, M. Wippler, R. Hranitzky, P. Gschwandtner, and T. Fahringer, "Multi-GPU room response simulation with hardware raytracing," *Concurrency and Computation: Practice and Experience*, vol. 34, no. 4, e6663, Feb. 2022, ISSN: 1532-0634. DOI: 10.1002/CPE.6663. [Online]. Available: https://onlinelibrary.wiley.com/doi/full/10.1002/cpe.6663%20https://onlinelibrary.wiley.com/doi/abs/10.1002/cpe.6663%20https://onlinelibrary.wiley.com/doi/10.1002/cpe.6663.

[11] F. Durán, A. Andrés, F. Grande, A. Figueroa-duran, and E. Fernandez-grande, *Reconstruction of room impulse responses over an extended spatial domain using block-sparse and kernel regression methods*, 2022. [Online]. Available: https://orbit.dtu.dk/en/publications/reconstruction-of-room-impulse-responses-over-an-extended-spatial.

[12] E. Fernandez-Grande, D. Caviedes-Nozal, M. Hahmann, X. Karakonstantis, and S. A. Verburg, "Reconstruction of room impulse responses over extended domains for navigable sound field reproduction," *2021 Immersive and 3D Audio: From Architecture to Automotive, I3DA 2021*, 2021. DOI: 10.1109/I3DA48870.2021.9610846.

[13] M. Pezzoli, D. Perini, A. Bernardini, F. Borra, F. Antonacci, and A. Sarti, "Deep Prior Approach for Room Impulse Response Reconstruction," *Sensors 2022, Vol. 22, Page 2710*, vol. 22, no. 7, p. 2710, Apr. 2022, ISSN: 1424-8220. DOI: 10.3390/S22072710. [Online]. Available: https://www.mdpi.com/1424-8220/22/7/2710/htm%20https://www.mdpi.com/1424-8220/22/7/2710.

[14] P. Masztalski, M. Matuszewski, K. Piaskowski, and M. Romaniuk, "StoRIR: Stochastic Room Impulse Response Generation for Audio Data Augmentation," *Proceedings of the Annual Conference of the International Speech Communication Association, INTERSPEECH*, vol. 2020-October, pp. 2857–2861, Aug. 2020, ISSN: 19909772. DOI: 10.21437/Interspeech.2020-2261. [Online]. Available: https://arxiv.org/abs/2008.07231v1.

[15] J. António, L. Godinho, and A. Tadeu, "Reverberation Times Obtained Using a Numerical Model Versus Those Given by Simplified Formulas and Measurements," Tech. Rep., 2002, pp. 252–261.

[16] A. F. Genovese, H. Gamper, V. Pulkki, N. Raghuvanshi, and I. J. Tashev, "Blind Room Volume Estimation from Single-channel Noisy Speech," *ICASSP, IEEE International Conference on Acoustics, Speech and Signal Processing - Proceedings*, vol. 2019-May, pp. 231–235, May 2019, ISSN: 15206149. DOI: 10.1109/ICASSP.2019.8682951.

[17] C. J. Steinmetz, V. K. Ithapu, and P. Calamia, "Filtered Noise Shaping for Time Domain Room Impulse Response Estimation from Reverberant Speech," *IEEE Workshop on Applications of Signal Processing to Audio and Acoustics*, vol. 2021-October, pp. 221–225, 2021, ISSN: 19471629. DOI: 10.1109/WASPAA52581.2021.9632680.

[18] L. Wang, Y. Lu, Z. Gao, *et al.*, "BERP: A Blind Estimator of Room Acoustic and Physical Parameters for Single-Channel Noisy Speech Signals," May 2024. [Online]. Available: https://arxiv.org/abs/2405.04476v2.

[19] S. Dilungana, A. Deleforge, C. Foy, and S. Faisan, "Geometry-Informed Estimation of Surface Absorption Profiles from Room Impulse Responses," *European Signal Processing Conference*, vol. 2022-August, pp. 867–871, 2022, ISSN: 22195491. DOI: 10.23919/EUSIPCO55093.2022.9909667.

[20] C. Bastien, A. Deleforge, and C. Foy, "Mean Absorption Coefficient Estimation From Impulse Responses: Deep Learning vs. Sabine," *Forum Acusticum*, no. 2, p. 2, Dec. 2020. DOI: 10.48465/FA.2020.0785. [Online]. Available: https://inria.hal.science/hal-03045556%20https://inria.hal.science/hal-03045556/document.

[21] P. Srivastava, A. Deleforge, and E. Vincent, "Blind Room Parameter Estimation Using Multiple Multichannel Speech Recordings," *IEEE Workshop on Applications of Signal Processing to Audio and Acoustics*, vol. 2021-October, pp. 226–230, 2023, ISSN: 19471629. DOI: 10.1109/WASPAA52581.2021.9632778.

[22] W. Yu, "The Estimation of Acoustic Parameters and Representations based on Room Impulse Responses," 2024. DOI: 10.4233/UUID:6923646E-09EA-4E06-9855-D3E487E5585F. [Online]. Available: https://repository.tudelft.nl/islandora/object/uuid%3A6923646e-09ea-4e06-9855-d3e487e5585f.

[23] C. Foy, A. Deleforge, D. D. Carlo, and C. Edric Foy, "Mean absorption estimation from room impulse responses using virtually supervised learning," *The Journal of the Acoustical Society of America*, vol. 150, no. 2, pp. 1286–1299, Aug. 2021, ISSN: 0001-4966. DOI: 10.1121/10.0005888. [Online]. Available: /asa/jasa/article/150/2/1286/615382/Mean-absorption-estimation-from-room-impulse.

[24] S. Dilungana, A. Deleforge, C. Foy, and S. Faisan, "Learning-based estimation of individual absorption profiles from a single room impulse response with known positions of source, sensor and surfaces," *INTER-NOISE and NOISE-CON Congress and Conference Proceedings*, vol. 263, no. 1, pp. 5623–5630, 2021, ISSN: 0736-2935. DOI: 10.3397/IN-2021-3186.

[25] W. Yu and W. B. Kleijn, "Room Acoustical Parameter Estimation from Room Impulse Responses Using Deep Neural Networks," *IEEE/ACM Transactions on Audio Speech and Language Processing*, vol. 29, pp. 436–447, 2021, ISSN: 23299304. DOI: 10.1109/TASLP.2020.3043115.

[26] P. Srivastava, A. Deleforge, and E. Vincent, "Blind room parameter estimation using multiple multichan-

nel speech recordings," Tech. Rep. [Online]. Available: https://hal.science/hal-03304656.

[27] D. P. Young, S. Stadler, K. W. Johnson, and J. D. Cutnell, "Cutnell & Johnson physics," p. 19, [Online]. Available: https://www.wiley.com/en-us/Physics%2C+12th+Edition-p-9781119773535R150.

[28] *NEN-EN-ISO 3382-2: Acoustics - Measurement of room acoustic parameters - Reverberation time in ordinairy rooms*. Delft: Nederlands Normalisatie-instituut, 2008. [Online]. Available: https://www.nen.nl/nen-en-iso-3382-2-2008-en-123846.

[29] M. T. Thompson, "Intuitive Analog Circuit Design, Second Edition," *Intuitive Analog Circuit Design, Second Edition*, pp. 1–697, Jan. 2013. DOI: 10.1016/C2012-0-03027-X. [Online]. Available: http://www.sciencedirect.com:5070/book/9780124058668/intuitive-analog-circuit-design.

[30] S. Ioffe and C. Szegedy, "Batch Normalization: Accelerating Deep Network Training by Reducing Internal Covariate Shift," *32nd International Conference on Machine Learning, ICML 2015*, vol. 1, pp. 448–456, Feb. 2015. [Online]. Available: https://arxiv.org/abs/1502.03167v3.

[31] T. O. Hodson, "Root-mean-square error (RMSE) or mean absolute error (MAE): when to use them or not," *Geoscientific Model Development*, vol. 15, no. 14, pp. 5481–5487, Jul. 2022, ISSN: 19919603. DOI: 10.5194/GMD-15-5481-2022.

[32] J. Qi, J. Du, S. M. Siniscalchi, X. Ma, and C.-H. Lee, "On Mean Absolute Error for Deep Neural Network Based Vector-to-Vector Regression," Aug. 2020. DOI: 10.1109/LSP.2020.3016837. [Online]. Available: http://arxiv.org/abs/2008.07281%20http://dx.doi.org/10.1109/LSP.2020.3016837.

[33] D. D. Carlo, P. Tandeitnik, C. Foy, N. Bertin, A. Deleforge, and S. Gannot, "dEchorate: a Calibrated Room Impulse Response Database for Echo-aware Signal Processing," *Eurasip Journal on Audio, Speech, and Music Processing*, vol. 2021, no. 1, Apr. 2021, ISSN: 16874722. DOI: 10.1186/s13636-021-00229-0. [Online]. Available: https://arxiv.org/abs/2104.13168v1.

[34] T. Houterman, "A design of an omnidirectional sound source used for impulse response measurements," TU Eindhoven, Tech. Rep., 2020, pp. 6–7.

[35] *NEN-EN-ISO 3382-1: Acoustics - Measurement of room acoustic parameters - Performance spaces*. Delft: Nederlandse Normalisatie-instituut, 2009. [Online]. Available: https://www.nen.nl/en/nen-en-iso-3382-1-2009-en-136495.

[36] M. R. Schroeder, "New method of measuring reverberation time," *The Journal of the Acoustical Society of America*, vol. 37, no. 6, pp. 1187–1188, 1965.

[37] K. Cox, "Model 831 Reverb time metrics (831-RT)," Tech. Rep.

[38] R. Scheibler, E. Bezzam, and I. Dokmanić, "Pyroomacoustics: A Python package for audio room simulations and array processing algorithms," *ICASSP, IEEE International Conference on Acoustics, Speech and Signal Processing - Proceedings*, vol. 2018-April, pp. 351–355, Oct. 2017. DOI: 10.1109/ICASSP.2018.8461310. [Online]. Available: http://arxiv.org/abs/1710.04196%20http://dx.doi.org/10.1109/ICASSP.2018.8461310.

[39] D. Diaz-Guerra, A. Miguel, and J. R. Beltran, "gpuRIR: A Python Library for Room Impulse Response Simulation with GPU Acceleration," *Multimedia Tools and Applications*, vol. 80, no. 4, pp. 5653–5671, Oct. 2018. DOI: 10.1007/s11042-020-09905-3. [Online]. Available: http://arxiv.org/abs/1810.11359%20http://dx.doi.org/10.1007/s11042-020-09905-3.

[40] E. Habets, *AudioLabs - RIR Generator*. [Online]. Available: https://www.audiolabs-erlangen.de/fau/professor/habets/software/rir-generator (visited on 06/16/2024).

[41] G. Guven, A. Arceo, A. Bennett, *et al.*, "A construction classification system database for understanding resource use in building construction," *Scientific Data 2022 9:1*, vol. 9, no. 1, pp. 1–12, Feb. 2022, ISSN: 2052-4463. DOI: 10.1038/s41597-022-01141-8. [Online]. Available: https://www.nature.com/articles/s41597-022-01141-8.

[42] Acoustic Traffic LLC, *Absorption Coefficients*. [Online]. Available: https://acoustic.ua/recommendations/800 (visited on 06/04/2024).

[43] P. Tol, *Paul Tol's Notes*. [Online]. Available: https://personal.sron.nl/~pault/ (visited on 06/18/2024).

APPENDIX

This appendix is an annotated version of an original dataset by Acoustic Traffic LLC [42]. These materials are used to model the materials of all the surfaces in the room simulations. The full process of modelling the materials is described in Section II-E. The annotations are made by the researcher. The categorization into reflective, wall, ceiling and floor is made based upon the material. If the average absorption coefficient of all frequency bands is less than 0.15, it categorizes as reflective. For non-obvious categorizations, the reasoning is in the notes.

Material	125	250	500	1000	2000	4000	Reflective	Wall	Floor	Ceiling	Excluded	Notes
Masonry walls												
Rough concrete	0.02	0.03	0.03	0.03	0.04	0.07	✓					
Smooth unpainted concrete	0.01	0.01	0.02	0.02	0.02	0.05	✓					
Smooth concrete, painted or glazed	0.01	0.01	0.01	0.02	0.02	0.02	✓					
Porous concrete blocks (no surface finish)	0.05	0.05	0.05	0.08	0.14	0.2	✓					
Clinker concrete (no surface finish)	0.1	0.2	0.4	0.6	0.5	0.6		✓				Outlier in the reflective set, maybe not representative?
Smooth brickwork with flush pointing	0.02	0.03	0.03	0.04	0.05	0.07	✓					
Smooth brickwork with flush pointing, painted	0.01	0.01	0.02	0.02	0.02	0.02	✓					
Standard brickwork	0.05	0.04	0.02	0.04	0.05	0.05	✓					
Brickwork, 10mm flush pointing	0.08	0.09	0.12	0.16	0.22	0.24		✓				Outlier in the reflective set, maybe not representative?
Lime cement plaster on masonry wall	0.02	0.02	0.03	0.04	0.05	0.05	✓					
Glaze plaster on masonry wall	0.01	0.01	0.01	0.02	0.02	0.02	✓					
Painted plaster surface on masonry wall	0.02	0.02	0.02	0.02	0.02	0.02	✓					
Plaster on masonry wall with wall paper on backing paper	0.02	0.03	0.04	0.05	0.07	0.08	✓					
Ceramic tiles with smooth surface	0.01	0.01	0.01	0.02	0.02	0.02	✓					
Breeze block	0.2	0.45	0.6	0.4	0.45	0.4		✓				
Plaster on solid wall	0.04	0.05	0.06	0.08	0.04	0.06	✓					
Plaster, lime or gypsum on solid backing	0.03	0.03	0.02	0.03	0.04	0.05	✓					
Studwork and lightweight walls												
Plasterboard on battens, 18mm airspace with glass wool	0.3	0.2	0.15	0.05	0.05	0.05	✓					
Plasterboard on frame, 100mm airspace	0.3	0.12	0.08	0.06	0.06	0.05	✓					
Plasterboard on frame, 100mm airspace wool	0.08	0.11	0.05	0.03	0.02	0.03	✓					
Plasterboard on 50mm battens	0.29	0.1	0.05	0.04	0.07	0.09	✓					High abs coef for lower frequencies
Plasterboard on 25mm battens	0.31	0.33	0.14	0.1	0.1	0.12		✓		✓		High abs coef for lower frequencies
2 x plasterboard on frame, 50mm airspace with mineral wool	0.15	0.1	0.06	0.04	0.04	0.05	✓					
Plasterboard on cellular core partition	0.15		0.07		0.04	0.05	✓					0 was removed at frequency 250 and 1000 Hz. This is due to suspicion of not having measured the material at these frequencies
Plasterboard on frame 100mm cavity	0.08	0.11	0.05	0.03	0.02	0.03	✓					
Plasterboard on frame, 100mm cavity with mineral wool	0.3	0.12	0.08	0.06	0.06	0.05	✓					
2 x 13mm plasterboard on steel frame, 50mm mineral wool in cavity, surface painted	0.15	0.01	0.06	0.04	0.04	0.05	✓					
Glass and glazing												
4mm glass	0.3	0.2	0.1	0.07	0.05	0.02	✓					
6mm glass	0.1	0.06	0.04	0.03	0.02	0.02	✓					
Double glazing, 2-3mm glass, 10mm air gap	0.15	0.05	0.03	0.03	0.02	0.02	✓					

Material	125	250	500	1000	2000	4000	Reflective	Wall	Floor	Ceiling	Excluded	Notes
Wood and wood panelling												
3-4mm plywood, 75mm cavity containing mineral wool	0.5	0.3	0.1	0.05	0.05	0.05		✓				
5mm plywood on battens, 50mm airspace filled	0.4	0.35	0.2	0.15	0.05	0.05		✓				
12mm plywood over 50mm airgap	0.25	0.05	0.04	0.03	0.03	0.02	✓					
12mm plywood over 150mm airgap	0.28	0.08	0.07	0.07	0.09	0.09	✓					
12mm plywood over 200mm airgap containing 50mm mineral wool	0.14	0.1	0.1	0.08	0.1	0.08	✓					
Plywood mounted solidly	0.05		0.05		0.05	0.05	✓					0 was removed at frequency 250 and 1000 Hz. This is due to suspicion of not having measured the material at these frequencies
12mm plywood in framework with 30mm airspace behind	0.35	0.2	0.15	0.1	0.05	0.05	✓					
12mm plywood in framework with 30mm airspace containing glass wool	0.4	0.2	0.15	0.1	0.1	0.05		✓				
Plywood, hardwood panels over 25mm airspace on solid backing	0.3	0.2	0.15	0.1	0.1	0.05	✓					
Plywood, hardwood panels over 25mm airspace on solid backing with absorbent material in air space	0.4	0.25	0.15	0.1	0.1	0.05		✓				
12mm wood panelling on 25mm battens	0.31	0.33	0.14	0.1	0.1	0.12		✓				
Timber boards, 100mm wide, 10mm gaps, 500mm airspace with mineral wool	0.05	0.25	0.6	0.15	0.05	0.1		✓				
t & g board on frame, 50mm airspace with mineral wool	0.25	0.15	0.1	0.09	0.08	0.07	✓					
16-22mm t&g wood on 50mm cavity filled with mineral wool	0.25	0.15	0.1	0.09	0.08	0.07	✓					
Cedar, slotted and profiled on battens mineral wool in airspace	0.2	0.62	0.98	0.62	0.21	0.15		✓				
Wood boards on on joists or battens	0.15	0.2	0.1	0.1	0.1	0.1	✓					
20mm dense veneered chipboard over 100mm airgap	0.03	0.05	0.04	0.03	0.03	0.02	✓					
20mm dense veneered chipboard over 200mm airgap	0.06	0.1	0.08	0.09	0.07	0.04	✓					
20mm dense veneered chipboard over 250mm airgap containing 50mm mineral wool	0.12	0.1	0.08	0.07	0.1	0.08	✓					
6mm wood fibre board, cavity ¿ 100mm, empty	0.3	0.2	0.2	0.1	0.05	0.05	✓					
22mm chipboard, 50mm cavity filled with mineral wool	0.12	0.04	0.06	0.05	0.05	0.05	✓					
Acoustic timber wall panelling	0.18	0.34	0.42	0.59	0.83	0.68		✓				
Hardwood, mahogany	0.19	0.23	0.25	0.3	0.37	0.42		✓				
Chipboard on 16mm battens	0.2	0.25	0.2	0.2	0.15	0.2		✓				

Material	125	250	500	1000	2000	4000	Reflective	Wall	Floor	Ceiling	Excluded	Notes
Chipboard on frame, 50mm airspace with mineral wool	0.12	0.04	0.06	0.05	0.05	0.05	✓					
Mineral wool and foams												
Melamine based foam 25mm	0.09	0.22	0.54	0.76	0.88	0.93		✓	✓	✓		Isolation can be applied on any surface
Melamine based foam 50mm	0.18	0.56	0.96	1	1	1		✓	✓	✓		Isolation can be applied on any surface
Glass wool 25mm 16 kg/m3	0.12	0.28	0.55	0.71	0.74	0.83		✓	✓	✓		Isolation can be applied on any surface
Glass wool 50mm, 16 kg/m3	0.17	0.45	0.8	0.89	0.97	0.94		✓	✓	✓		Isolation can be applied on any surface
Glass wool 75mm, 16 kg/m3	0.3	0.69	0.94	1	1	1		✓	✓	✓		Isolation can be applied on any surface
Glass wool 100mm, 16 kg/m3	0.43	0.86	1	1	1	1		✓	✓	✓		Isolation can be applied on any surface
Glass wool 25mm, 24 kg/m3	0.11	0.32	0.56	0.77	0.89	0.91		✓	✓	✓		Isolation can be applied on any surface
Glass wool 50mm, 24 kg/m3	0.27	0.54	0.94	1	0.96	0.96		✓	✓	✓		Isolation can be applied on any surface
Glass wool 75mm, 24 kg/m3	0.28	0.79	1	1	1	1		✓	✓	✓		Isolation can be applied on any surface
Glass wool 100mm, 24 kg/m3	0.46	1	1	1	1	1		✓	✓	✓		Isolation can be applied on any surface
Glass wool 50mm, 33 kg/m3	0.2	0.55	1	1	1	1		✓	✓	✓		Isolation can be applied on any surface
Glass wool 75mm, 33 kg/m3	0.37	0.85	1	1	1	1		✓	✓	✓		Isolation can be applied on any surface
Glass wool 100mm, 33 kg/m3	0.53	0.92	1	1	1	1		✓	✓	✓		Isolation can be applied on any surface
Glass wool 50mm, 48 kg/m3	0.3	0.8	1	1	1	1		✓	✓	✓		Isolation can be applied on any surface
Glass wool 75mm, 48 kg/m3	0.43	0.97	1	1	1	1		✓	✓	✓		Isolation can be applied on any surface
Glass wool 100mm, 48 kg/m3	0.65	1	1	1	1	1		✓	✓	✓		Isolation can be applied on any surface
Rock wool 50mm, 33 kg/m3 direct to masonry	0.15	0.6	0.9	0.9	0.9	0.85		✓	✓	✓		Isolation can be applied on any surface
Rock wool 100mm, 33 kg/m3 direct to masonry	0.35	0.95	0.98	0.92	0.9	0.85		✓	✓	✓		Isolation can be applied on any surface
Rock wool 50mm, 60 kg/m3 direct to masonry	0.11	0.6	0.96	0.94	0.92	0.82		✓	✓	✓		Isolation can be applied on any surface
Rock wool 75mm, 60 kg/m3 direct to masonry	0.34	0.95	0.98	0.82	0.87	0.86		✓	✓	✓		Isolation can be applied on any surface
Rock wool 30mm, 100 kg/m3 direct to masonry	0.1	0.4	0.8	0.9	0.9	0.9		✓	✓	✓		Isolation can be applied on any surface
Rock wool 30mm, 200 kg/m3 over 300mm air gap	0.4	0.75	0.9	0.8	0.9	0.85		✓	✓	✓		Isolation can be applied on any surface
Glass wool or mineral wool on solid backing	0.2		0.7		0.9	0.8		✓	✓	✓		Isolation can be applied on any surface. 0 was removed at frequency 250 and 1000 Hz. This is due to suspicion of not having measured the material at these frequencies
Glass wool or mineral wool on solid backing	0.3		0.8		0.95	0.9		✓	✓	✓		Isolation can be applied on any surface. 0 was removed at frequency 250 and 1000 Hz. This is due to suspicion of not having measured the material at these frequencies
Glass wool or mineral wool over air space on solid backing	0.4		0.8		0.9	0.8		✓	✓	✓		Isolation can be applied on any surface. 0 was removed at frequency 250 and 1000 Hz. This is due to suspicion of not having measured the material at these frequencies
Fibreglass super fine mat	0.15	0.4	0.75	0.85	0.8	0.85		✓	✓	✓		Isolation can be applied on any surface

Material	125	250	500	1000	2000	4000	Reflective	Wall	Floor	Ceiling	Excluded	Notes
Fibreglass scrim-covered sewn sheet	0.4	0.8	0.95	0.95	0.8	0.85		✓	✓	✓		Isolation can be applied on any surface
Fibreglass bitumen bonded mat	0.1	0.35	0.5	0.55	0.7	0.7		✓	✓	✓		Isolation can be applied on any surface
Fibreglass bitumen bonded mat	0.3	0.55	0.8	0.85	0.75	0.8		✓	✓	✓		Isolation can be applied on any surface
Fibreglass resin-bonded mat	0.1	0.35	0.55	0.65	0.75	0.8		✓	✓	✓		Isolation can be applied on any surface
Fibreglass resin-bonded mat	0.2	0.5	0.7	0.8	0.75	0.8		✓	✓	✓		Isolation can be applied on any surface
Fibreglass resin-bonded board	0.1	0.25	0.55	0.7	0.8	0.85		✓	✓	✓		Isolation can be applied on any surface
Flexible polyurethane foam 50mm	0.25	0.5	0.85	0.95	0.9	0.9		✓	✓	✓		Isolation can be applied on any surface
Rigid polyurethane foam 50mm	0.2	0.4	0.65	0.55	0.7	0.7		✓	✓	✓		Isolation can be applied on any surface
12mm expanded polystyrene on 45mm battens	0.05	0.15	0.4	0.35	0.2	0.2		✓	✓	✓		Isolation can be applied on any surface
25mm expanded polystyrene on 50mm battens	0.1	0.25	0.55	0.2	0.1	0.15		✓	✓	✓		Isolation can be applied on any surface
Wall treatments & Constructions												
Cork tiles 25mm on solid backing	0.05	0.1	0.2	0.55	0.6	0.55		✓		✓		While maybe unconventional, these materials are light and don't support the main construction of a building. It is possible to mount them on a ceiling
Cork board, 25mm on solid backing	0.03	0.05	0.17	0.52	0.5	0.52		✓		✓		While maybe unconventional, these materials are light and don't support the main construction of a building. It is possible to mount them on a ceiling
Cork board, 25mm, 2.9kg/m2, on battens	0.15	0.4	0.65	0.35	0.35	0.3		✓		✓		While maybe unconventional, these materials are light and don't support the main construction of a building. It is possible to mount them on a ceiling
Glass blocks or glazed tiles as wall finish	0.01		0.01		0.01	0.01	✓					0 was removed at frequency 250 and 1000 Hz. This is due to suspicion of not having measured the material at these frequencies
Muslin covered cotton felt	0.15	0.45	0.7	0.85	0.95	0.85		✓		✓		While maybe unconventional, these materials are light and don't support the main construction of a building. It is possible to mount them on a ceiling
Pin up boarding- medium hardboard on solid backing	0.05		0.1		0.1	0.1	✓					0 was removed at frequency 250 and 1000 Hz. This is due to suspicion of not having measured the material at these frequencies
Fibreboard on solid backing	0.05	0.1	0.15	0.25	0.3	0.3		✓		✓		While maybe unconventional, these materials are light and don't support the main construction of a building. It is possible to mount them on a ceiling

Material	125	250	500	1000	2000	4000	Reflective	Wall	Floor	Ceiling	Excluded	Notes
25mm thick hair felt, covered by scrim cloth on solid backing	0.1		0.7		0.8	0.8		✓		✓		While maybe unconventional, these materials are light and don't support the main construction of a building. It is possible to mount them on a ceiling. 0 was removed at frequency 250 and 1000 Hz. This is due to suspicion of not having measured the material at these frequencies
Fibreboard on solid backing	0.05		0.15		0.3	0.3		✓		✓		While maybe unconventional, these materials are light and don't support the main construction of a building. It is possible to mount them on a ceiling. 0 was removed at frequency 250 and 1000 Hz. This is due to suspicion of not having measured the material at these frequencies
Fibreboard on solid backing - painted	0.05		0.1		0.15	0.15	✓					0 was removed at frequency 250 and 1000 Hz. This is due to suspicion of not having measured the material at these frequencies
Fibreboard over airspace on solid wall	0.3		0.3		0.3	0.3		✓		✓		While maybe unconventional, these materials are light and don't support the main construction of a building. It is possible to mount them on a ceiling. 0 was removed at frequency 250 and 1000 Hz. This is due to suspicion of not having measured the material at these frequencies
Fibreboard over airspace on solid wall - painted	0.3		0.15		0.1	0.1		✓		✓		While maybe unconventional, these materials are light and don't support the main construction of a building. It is possible to mount them on a ceiling. 0 was removed at frequency 250 and 1000 Hz. This is due to suspicion of not having measured the material at these frequencies
Plaster on lath, deep air space	0.2	0.15	0.1	0.05	0.05	0.05	✓					
Plaster decorative panels, walls	0.2	0.15	0.1	0.08	0.04	0.02	✓					
Acoustic plaster to solid backing	0.03	0.15	0.5	0.8	0.85	0.8		✓		✓		While maybe unconventional, these materials are light and don't support the main construction of a building. It is possible to mount them on a ceiling
9mm acoustic plaster to solid backing	0.02	0.08	0.3	0.6	0.8	0.9		✓		✓		While maybe unconventional, these materials are light and don't support the main construction of a building. It is possible to mount them on a ceiling

Material	125	250	500	1000	2000	4000	Reflective	Wall	Floor	Ceiling	Excluded	Notes
9mm acoustic plaster on plasterboard, 75mm airspace	0.3	0.3	0.6	0.8	0.75	0.75		✓		✓		While maybe unconventional, these materials are light and don't support the main construction of a building. It is possible to mount them on a ceiling
12.5mm acoustic plaster on plaster backing over 75mm air space	0.35	0.35	0.4	0.55	0.7	0.7		✓		✓		While maybe unconventional, these materials are light and don't support the main construction of a building. It is possible to mount them on a ceiling
Woodwool slabs, unplastered on solid backing	0.1		0.4		0.6	0.6		✓		✓		While maybe unconventional, these materials are light and don't support the main construction of a building. It is possible to mount them on a ceiling. 0 was removed at frequency 250 and 1000 Hz. This is due to suspicion of not having measured the material at these frequencies
Woodwool slabs, unplastered on solid backing	0.1	0.2	0.45	0.8	0.6	0.75		✓		✓		While maybe unconventional, these materials are light and don't support the main construction of a building. It is possible to mount them on a ceiling
Woodwool slabs, unplastered on solid backing	0.2		0.8		0.8	0.8		✓		✓		While maybe unconventional, these materials are light and don't support the main construction of a building. It is possible to mount them on a ceiling. 0 was removed at frequency 250 and 1000 Hz. This is due to suspicion of not having measured the material at these frequencies
Woodwool slabs, unplastered over 20mm airspace on solid backing	0.15		0.6		0.6	0.7		✓		✓		While maybe unconventional, these materials are light and don't support the main construction of a building. It is possible to mount them on a ceiling. 0 was removed at frequency 250 and 1000 Hz. This is due to suspicion of not having measured the material at these frequencies
Plasterboard backed with 25mm thick bitumen-bonded fibreglass on 50mm battens	0.3	0.2	0.15	0.05	0.05	0.05	✓					
Curtains hung in folds against soild wall	0.05	0.15	0.35	0.4	0.5	0.5		✓				
Cotton Curtains (0.5kg/m2),draped to 75% area approx. 130mm from wall	0.3	0.45	0.65	0.56	0.59	0.71		✓				
Lightweight curtains (0.2 kg/m2) hung 90mm from wall	0.05	0.06	0.39	0.63	0.7	0.73		✓				
Curtains of close-woven glass mat hung 50mm from wall	0.03	0.03	0.15	0.4	0.5	0.5		✓				

Material	125	250	500	1000	2000	4000	Reflective	Wall	Floor	Ceiling	Excluded	Notes
Curtains, medium velour, 50% gather, over solid backing	0.05	0.25	0.4	0.5	0.6	0.5		✓				
Curtains (medium fabrics) hung straight and close to wall	0.05		0.25		0.3	0.4		✓				0 was removed at frequency 250 and 1000 Hz. This is due to suspicion of not having measured the material at these frequencies
Curtains in folds against wall	0.05	0.15	0.35	0.4	0.5	0.5		✓				
Curtains (medium fabrics) double widths in folds spaced away from wall	0.1		0.4		0.5	0.6		✓				0 was removed at frequency 250 and 1000 Hz. This is due to suspicion of not having measured the material at these frequencies
Acoustic banner, 0.5 kg/m2 wool serge, 100mm from wall	0.11	0.4	0.7	0.74	0.88	0.89		✓		✓		While maybe unconventional, these materials are light and don't support the main construction of a building. It is possible to mount them on a ceiling
Floors												
Smooth marble or terrazzo slabs	0.01	0.01	0.01	0.01	0.02	0.02	✓					
Raised computer floor, steel-faced 45mm chipboard 800mm above concrete floor, no carpet	0.08	0.07	0.06	0.07	0.08	0.08	✓					
Raised computer floor, steel-faced 45mm chipboard 800mm above concrete floor, office-grade carpet tiles	0.27	0.26	0.52	0.43	0.51	0.58			✓			
Wooden floor on joists	0.15	0.11	0.1	0.07	0.06	0.07	✓					
Parquet fixed in asphalt, on concrete	0.04	0.04	0.07	0.06	0.06	0.07	✓					
Parquet on counterfloor	0.2	0.15	0.1	0.1	0.05	0.1	✓					
Linoleum or vinyl stuck to concrete	0.02	0.02	0.03	0.04	0.04	0.05	✓					
Layer of rubber, cork, linoleum + underlay, or vinyl+underlay stuck to concrete	0.02	0.02	0.04	0.05	0.05	0.1	✓					
5mm needle-felt stuck to concrete	0.01	0.02	0.05	0.15	0.3	0.4			✓			
6mm pile carpet bonded to closed-cell foam underlay	0.03	0.09	0.25	0.31	0.33	0.44			✓			
6mm pile carpet bonded to open-cell foam underlay	0.03	0.09	0.2	0.54	0.7	0.72			✓			
9mm pile carpet, tufted on felt underlay	0.08	0.08	0.3	0.6	0.75	0.8			✓			
Composition flooring	0.05	0.05	0.05	0.05	0.05	0.05	✓					
Haircord carpet on felt underlay	0.05	0.05	0.1	0.2	0.45	0.65			✓			
Medium pile carpet on sponge rubber underlay	0.5	0.1	0.3	0.5	0.65	0.7			✓			
Thick pile carpet on sponge rubber underlay	0.15	0.25	0.5	0.6	0.7	0.7			✓			
Rubber floor tiles	0.05	0.05	0.1	0.1	0.05	0.05	✓					
Carpet, thin, over thin felt on concrete	0.1	0.15	0.25	0.3	0.3	0.3			✓			
Carpet, thin, over thin felt on wood floor	0.2	0.25	0.3	0.3	0.3	0.3			✓			
Carpet, needlepunch	0.03	0.05	0.05	0.25	0.35	0.5			✓			

Material	125	250	500	1000	2000	4000	Reflective	Wall	Floor	Ceiling	Excluded	Notes
Stone floor, plain or tooled or granolithic finish	0.02		0.02		0.05	0.05	✓					0 was removed at frequency 250 and 1000 Hz. This is due to suspicion of not having measured the material at these frequencies
Corkfloor tiles		0.05	0.15	0.25	0.25				✓			0 values removed at frequency range 125 and 4000. This is due to the suspicion that there was no measurement at that frequency range.
Sheet rubber (hard)		0.05	0.05	0.1	0.05		✓					0 values removed at frequency range 125 and 4000. This is due to the suspicion that there was no measurement at that frequency range.
Woodblock/linoleum/rubber/cork tiles (thin) on solid floor (or wall)	0.02	0.04	0.05	0.05	0.1	0.05	✓					
Floor tiles, plastic or linoleum	0.03		0.03		0.05	0.05	✓					0 was removed at frequency 250 and 1000 Hz. This is due to suspicion of not having measured the material at these frequencies
Steel decking	0.13	0.09	0.08	0.09	0.11	0.11	✓					
Panels and doors												
Wood hollowcore door	0.3	0.25	0.15	0.1	0.1	0.07		✓				
Solid timber door	0.14	0.1	0.06	0.08	0.1	0.1	✓					
Acoustic door, steel frame, double seals, absorbant in airspace, Double sheet steel skin.	0.35	0.39	0.44	0.49	0.54	0.57		✓				
Ceilings												
Mineral wool tiles, 180mm airspace	0.42	0.72	0.83	0.88	0.89	0.8				✓		
Mineral wool tiles, glued/screwed to soffit	0.06	0.4	0.75	0.95	0.96	0.83				✓		
Gypsum plaster tiles, 17% perforated, 22mm	0.45	0.7	0.8	0.8	0.65	0.45				✓		
Metal ceiling, 32.5% perforated, backed by 30mm rockwool	0.12	0.45	0.87	0.98	1	1				✓		
Perforated underside of structural steel decking (typical, depends on perforations)	0.3	0.7	0.85	0.9	0.7	0.65				✓		
12% perforated plaster tiles, absorbent felt glued to back, 200mm ceiling void	0.45	0.7	0.88	0.52	0.42	0.35				✓		
100mm woodwool slabs on 25mm cavity, prescreeded surface facing cavity	0.5	0.75	0.85	0.65	0.7	0.7				✓		
50mm woodwool slabs on 25mm cavity, prescreeded surface facing cavity	0.3	0.4	0.5	0.85	0.5	0.65				✓		
100mm woodwool fixed directly to concrete, prescreeded surface facing backing	0.25	0.8	0.85	0.65	0.7	0.75				✓		
75mm woodwool fixed directly to concrete, prescreeded surface facing backing	0.15	0.4	0.95	0.6	0.7	0.6				✓		
Plasterboard 10mm thick backed with 25mm thick bitumen	0.3	0.2	0.15	0.05	0.05	0.05	✓					

Material	125	250	500	1000	2000	4000	Reflective	Wall	Floor	Ceiling	Excluded	Notes
Plasterboard 10mm thick, perforated 8mm diameter holes 2755m2 14% open area backed with 25mm thick bitumen- bonded fibreglass on 90mm battens	0.25	0.7	0.85	0.55	0.4	0.3				✓		
Plywood, 5mm, on battens 50mm airspace filled with glass wool	0.4	0.35	0.2	0.15	0.05	0.05				✓		
Plywood, 12mm, with 30mm thick fibreglass backing between 30mm battens	0.4	0.2	0.15	0.1	0.1	0.05				✓		
Plywood 12mm thick perforated 5mm diameter holes 6200 m2 11% open area with 60mm deep air space behind	0.2	0.35	0.55	0.3	0.25	0.3				✓		
Plywood 12mm thick perforated 5mm diameter holes 6200 m2 11% open area backed with 60mm thick fibreglass between mounting battens	0.4	0.9	0.8	0.5	0.4	0.3				✓		
Hardboard, 25% perforated over 50mm mineral wool	0.27	0.87	1	1	0.98	0.96				✓		
0.8mm unperforated metal panels backed with 25mm thick resin bonded fibreglass, mounted on 22mm diameter pipes 135mm from wall.	0.5	0.35	0.15	0.05	0.05					✓		0 values removed at frequency range 4000. This is due to the suspicion that there was no measurement at that frequency range.
0.8mm perforated metal tiles 2mm diameter holes 29440/m2. 13% open area backed with 25mm thick resin-bonded fibreglass slab. No airspace.	0.1	0.3	0.6	0.75	0.8	0.8				✓		
50mm mineral wool (96 kg/m3) behind 25% open area perforated steel.	0.2	0.35	0.65	0.85	0.9	0.8				✓		
Wood panels, 18mm alternate 15mm slot & 35mm wooden slat	0.1	0.36	0.74	0.91	0.61	0.5				✓		
25mm rockwool backing, 32mm airspace behind Plaster decorative panels, ceilings	0.2	0.22	0.18	0.15	0.15	0.16				✓		
Audience and seating												
Children, standing (per child) in m2 units	0.12	0.22	0.37	0.4	0.42	0.37					✓	We will only consider empty rooms for this study.
Children, seated in plastic or metal chairs (per child) in m2 units	0.28		0.33		0.37	0.37					✓	We will only consider empty rooms for this study.
Students seated in tablet arm chairs	0.3	0.41	0.49	0.84	0.87	0.84					✓	We will only consider empty rooms for this study.
Adults per person seated	0.33	0.4	0.44	0.45	0.45	0.45					✓	We will only consider empty rooms for this study.
Adults per person standing	0.15	0.38	0.42	0.43	0.45	0.45					✓	We will only consider empty rooms for this study.
Empty plastic or metal chairs (per chair) in m2 units	0.07		0.14		0.14	0.14					✓	We will only consider empty rooms for this study.
Seats, leather covers, per m2	0.4	0.5	0.58	0.61	0.58	0.5					✓	We will only consider empty rooms for this study.

Material	125	250	500	1000	2000	4000	Reflective	Wall	Floor	Ceiling	Excluded	Notes
Cloth-upholstered seats, per m2	0.44	0.6	0.77	0.89	0.82	0.7					✓	We will only consider empty rooms for this study.
Floor and cloth-upholstered seats, per m2	0.49	0.66	0.8	0.88	0.82	0.7					✓	We will only consider empty rooms for this study.
Adults in plastic and metal chairs in m2 units	0.3	0	0.4	0	0.43	0.4					✓	We will only consider empty rooms for this study.
Adults in wooden or padded chairs or seats (per item) in m2	0.16	0	0.4	0	0.44	0.4					✓	We will only consider empty rooms for this study.
Adults on timber seats, 1 per m2 per item	0.16	0.24	0.56	0.69	0.81	0.78					✓	We will only consider empty rooms for this study.
Adults on timber seats, 2 per m2 per item	0.24	0.4	0.78	0.98	0.96	0.87					✓	We will only consider empty rooms for this study.
Wooden or padded chairs or seats (per item) in m2	0.08	0	0.15	0	0.18	0.2					✓	We will only consider empty rooms for this study.
Seating, slighty upholstered, unoccupied	0.07	0.12	0.26	0.42	0.5	0.55					✓	We will only consider empty rooms for this study.
Seating, slighty upholstered, occupied	0.32	0.62	0.74	0.76	0.81	0.9					✓	We will only consider empty rooms for this study.
Fully upholstered seats (per item) in m2	0.12	0	0.28	0	0.32	0.37					✓	We will only consider empty rooms for this study.
Upholstered tip-up theatre seats, empty	0.33	0.51	0.64	0.71	0.77	0.81					✓	We will only consider empty rooms for this study.
Areas with audience, orchestra, or seats, including narrow aisles	0.6	0.74	0.88	0.96	0.93	0.85					✓	We will only consider empty rooms for this study.
Auditorium seat, unoccupied	0.13	0.33	0.59	0.58	0.61	0.62					✓	We will only consider empty rooms for this study.
Auditorium seat, occupied	0.37	0.48	0.68	0.73	0.77	0.74					✓	We will only consider empty rooms for this study.
Orchestra with instruments on podium, 1.5 m2 per person	0.27	0.53	0.67	0.93	0.87	0.8					✓	We will only consider empty rooms for this study.
Orchestral player with instrument (average) per person	0.37	0.8	1	1	1	1					✓	We will only consider empty rooms for this study.
Prosenium opening with average stage set per m2 of opening	0.2	0	0.3	0	0.4	0.5					✓	We will only consider empty rooms for this study.
Wood platform with large space beneath	0.4	0.3	0.2	0.17	0.15	0.1					✓	We will only consider empty rooms for this study.
Adult office furniture per desk	0.5	0.4	0.45	0.45	0.6	0.7					✓	We will only consider empty rooms for this study.
Other												
Water surface, ie swimming pool	0.01	0.01	0.01	0.01	0.02	0.02					✓	We exclude pools inside.
Ventilation grille per m2	0.6	0.6	0.6	0.6	0.6	0.6					✓	This is too niche for a generic material